JOURNAL OF Applied Polymer SCIENCE

Thermal Decomposition Studies of Schiff-Base-Substitute Polyphenol-Metal Complexes

Fatih Doğan,[1] İsmet Kaya[1,2]

[1]Çanakkale Onsekiz Mart University, Faculty of Education, Secondary Science and Mathematics Education 17100, Çanakkale, Turkey

[2]Çanakkale Onsekiz Mart University, Faculty of Arts and Science, Department of Chemistry, Çanakkale, Turkey

Correspondence to: F. Doğan (E-mail: fatih.dogan@ege.edu.tr)

ABSTRACT: The thermal behaviors of 2,3-bis[(2-hydroxyphenyl)methylene] diaminopyridine, oligo-2,3-bis[(2-hydroxyphenyl)methylene] diaminopyridine, and some oligo-2,3-bis[(2-hydroxyphenyl) methylene] diaminopyridine–metal complexes were studied in a nitrogen atmosphere with thermogravimetric analysis, derivative thermogravimetric analysis, and differential thermal analysis techniques. The decompositions of oligo-2,3-bis[(2-hydroxyphenyl) methylene] diamino pyridine–metal complexes occurred in multiple steps. The values of the activation energy (E) and reaction order of the thermal decomposition were calculated by means of several methods, including Coats–Redfern, Horowitz–Metzger, Madhusudanan–Krishnan–Ninan, van Krevelen, Wanjun–Yuwen–Hen–Cunxin, and MacCallum–Tanner on the basis of a single heating rate. The most appropriate method was determined for each decomposition step according to a least-squares linear regression. The E values obtained by each method were in good agreement with each other. It was found that the E values of the complexes for the first decomposition stage followed the order $E_{OHPMDAP–Ni} > E_{OHPMDAP–Cd} > E_{OHPMDAP–Cu} > E_{OHPMDAP–Fe} > E_{OHPMDAP–Zn} > E_{OHPMDAP–Co} > E_{OHPMDAP–Cr} > E_{HPMDAP} > E_{OHPMDAP}$. © 2012 Wiley Periodicals, Inc. J. Appl. Polym. Sci. 128: 3782–3793, 2013

KEYWORDS: activation energy; thermal properties; thermodynamics

revised 11 July 2012; accepted 19 July 2012; published online 12 October 2012

DOI: 10.1002/app.38392

INTRODUCTION

In recent years, polymer–metal complexes have been of interest to many chemists because of their potential important application, such as adhesives, high-temperature lubricants, electrical insulators, and semiconductors.[1–5] They have good thermal stability because of their rigid main chain. So, the thermal properties of Schiff-base polymer–metal complexes have been studied widely. Copper(II)-chelated polyazomethines were synthesized, and the influence of the copper content on the thermal behavior was studied by Oriol et al.[6] Thermally stable Schiff-base polymers and their metal(II) complexes were reported by Mart.[7] Schiff-base substitute oligo/polyphenol–metal complexes and their thermal properties were examined by Kaya and coworkers.[8–10]

In this study, the thermal properties and decomposition kinetics of 2,3-bis[(2-hydroxyphenyl)methylene] diaminopyridine (HPMDAP), oligo-2,3-bis[(2-hydroxyphenyl) methylene] diaminopyridine (OHPMDAP), and oligo-2,3-bis[(2-hydroxyphenyl)-methylene] diaminopyridine–metal complexes (OHPMDAP–M) of Zn(II), Pb(II), Ni(II), Cr(III), Fe(II), Cu(II), Co(II), and Cd(II) were investigated. In the decomposition kinetic study, methods such as Coats–Redfern (CR),[11] Horowitz–Metzger (HM),[12] Madhusudanan–Krishnan–Ninan (MKN),[13] van Krevelen (vK),[14] Wanjun–Yuwen–Hen–Cunxin (WYHC),[15] and MacCallum–Tanner (MT)[16] were used for the calculation of kinetic parameters such as the reaction order (n), the activation energy (E), entropy change of activation ($\Delta S^{\#}$), enthalpy change of activation ($\Delta H^{\#}$), Gibbs free energy change of activation ($\Delta G^{\#}$), and pre-exponential factor (A). The mechanism function related to the each thermal decomposition process was also investigated by Criado–Malek–Ortega method.[17]

EXPERIMENTAL

Materials

All of the compounds and solvents used were supplied from Merck Chemical Co. (Germany) Sodium hypochloride (NaOCl; 30% aqueous solution) was supplied from Paksoy Chemical Co. (Adana, Turkey).

Preparation of the HPMDAP, OHPMDAP, and OHPMDAP–Metal Complexes

The HPMDAP, OHPMDAP, and OHPMDAP–metal complex compounds were prepared according to reported procedures.[18] HPMDAP was prepared by the condensation of salicylaldehyde (1.22 g, 0.01 mol) and 2,3-diaminopyridine (0.55 g, 0.005 mol) in methanol (15 mL) achieved by the boiling of the mixture under

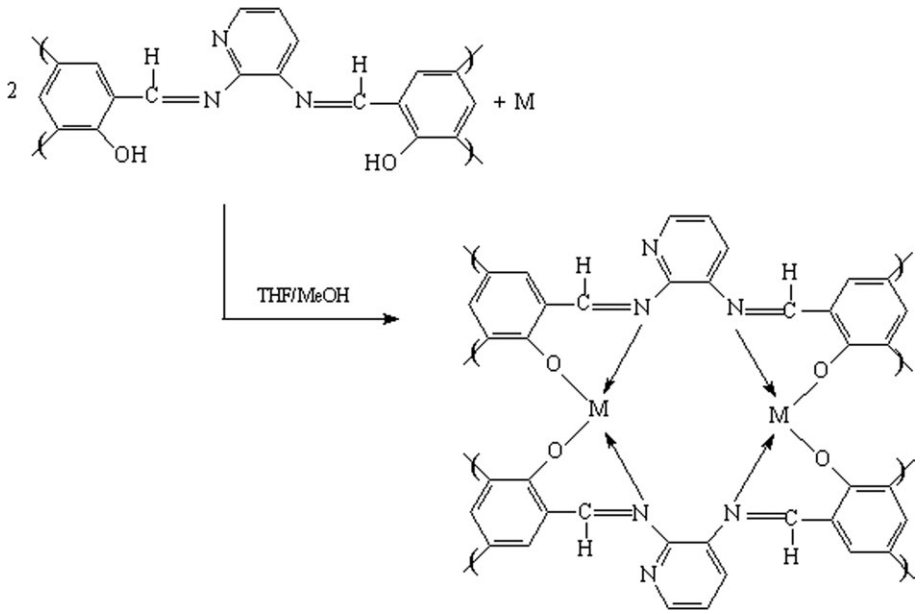

Scheme 1. Syntheses of the oligomer–metal complex compounds [M = Ni(II), Cd(II), Cu(II), Fe(II), Zn(II), Co(II), Cr(III), or Pb(II)].

reflux for 3 h. The precipitated HPMDAP was filtered and recrystallized from methanol and dried in vacuum desiccators (yield = 78%). OHPMDAP was synthesized from the oxidative polycondensation reaction of HPMDAP with an aqueous solution of NaOCl (30%). A solution of $Co(AcO)_2{\cdot}4H_2O$, $Ni(AcO)_2{\cdot}4H_2O$, $Cu(AcO)_2{\cdot}H_2O$, $FeSO_4{\cdot}7H_2O$, $Zn(AcO)_2{\cdot}2H_2O$, $Pb(AcO)_2{\cdot}3H_2O$, $CrCl_3{\cdot}6H_2O$, and $Cd(AcO)_2{\cdot}2H_2O$ (2 mmol) in methanol (10 mL) was added to a solution of OHPMDAP (2 mmol/unit) in tetrahydrofuran (THF; 20 mL). The mixture was stirred for 3 h at room temperature (Scheme 1). The precipitated complex was filtered, washed with cold methanol/THF (1:1), and then dried in a vacuum oven.

Kinetic Parameters

The six methods investigated in this study were the MKN, MT, WHYC, vK, CR, and HM methods.

The equation for the MKN method is as follows:

$$\ln\left[\frac{g(\alpha)}{T^{1.9206}}\right] = \ln\left(\frac{AE}{\beta R}\right) + 3.7678 - 1.9206\ln E - 0.12040\left(\frac{E}{T}\right) \quad (1)$$

The equation for the MT method is as follows:

$$\log g\left(\alpha\right) = \log\left(\frac{AE}{\beta R}\right) - 0.4828E^{0.4351} - \left(\frac{0.449 + 0.217E}{10^{-3}T}\right) \quad (2)$$

The equation for the WYHC method is as follows:

$$\ln\left[\frac{g(\alpha)}{T^{1.8946}}\right] = \left[\ln\frac{AR}{\beta E} + 3.6350 - 1.8946\ln E\right] - 1.0014\left(\frac{E}{RT}\right) \quad (3)$$

The equation for the vK method is as follows:

$$\ln g(\alpha) = \ln\left[\frac{A(0.368/T_m)^{\frac{E_a}{RT_m}}}{\beta(\frac{E_a}{RT_m}+1)}\right] + \left(\frac{E_a}{RT_m}+1\right)\ln T \quad (4)$$

The equation for the CR method is as follows:

$$\ln\left[\frac{g(\alpha)}{T^2}\right] = \ln\left[\frac{AR}{\beta E}\left(1-\frac{2RT}{E}\right)\right] - \left(\frac{E}{RT}\right) \quad (5)$$

where n is reaction order.

The HM method introduced a characteristic temperature (T_m) and a parameter θ such that

$$\theta = T - T_m$$

If n is 1, T_m is defined as the temperature at which $(1-\alpha)_m = 1/e = 0.368$, and the final expression is

$$\ln\ln g(\alpha) = \frac{E\theta}{RT_m^2}$$

where α is reaction degree.

If n is unknown, T_m is defined by the maximum heating rate.

When θ = 0, $(1-\alpha) = (1-\alpha)_m$, and $(1-\alpha)_m = n^{1/1-n}$ and

$$\ln\left[\frac{1-(1-\alpha)^{1-n}}{(1-n)}\right] = \ln\frac{ART_m^2}{\beta E} - \frac{E}{RT_m} + \frac{E\theta}{RT_m^2} \quad (6)$$

In the Criado–Malek–Ortega method, if the value of E is known, the kinetic model of the process can be determined by this method. Criado et al.[17] defined the function as follows:

$$z(\alpha) = \frac{\left(\frac{d\alpha}{dt}\right)}{\beta}\pi(x)\,T \quad (7)$$

where $x = E/RT$ and $\pi(x)$ is an approximation of the temperature integral, which cannot be expressed in a simple analytical form. In this case, the fourth rational expression of Senum and Yang[19] has been used. Combining a rate expression, $\frac{d\alpha}{dt} = kf(\alpha)$, and eq. (7), we can obtain

$$z(\alpha) = f(\alpha)F(\alpha) \quad (8)$$

where $F(\alpha)$ is function dependent of the real reation mechanism and $Z(\alpha)$ is function of reaction degree.

Table I. Algebraic Expressions for the Most Frequently used Mechanisms of Solid-State Processes

Number	Mechanism	Symbol	Differential form [$f(\alpha)$]	Integral form [$g(\alpha)$]
Sigmoidal curves				
1	N and G ($n = 1$)	A_1	$(1-\alpha)$	$[-\ln(1-\alpha)]$
2	N and G ($n = 1.5$),	$A_{1.5}$	$(3/2)(1-\alpha)[-\ln(1-\alpha)]^{1/3}$	$[-\ln(1-\alpha)]^{2/3}$
3	N and G ($n = 2$)	A_2	$2(1-\alpha)[-\ln(1-\alpha)]^{1/2}$	$[-\ln(1-\alpha)]^{1/2}$
4	N and G ($n = 3$),	A_3	$3(1-\alpha)[-\ln(1-\alpha)]^{2/3}$	$[-\ln(1-\alpha)]^{1/3}$
5	N and G ($n = 4$),	A_4	$4(1-\alpha)[-\ln(1-\alpha)]^{3/4}$	$[-\ln(1-\alpha)]^{1/4}$
Deceleration curves				
6	Diffusion, one-dimensional	D_1	$1/(2\,\alpha)$	α^2
7	Diffusion, two-dimensional	D_2	$1/(\ln(1-\alpha))$	$(1-\alpha)\ln(1-\alpha)+\alpha$
8	Diffusion, three-dimensional	D_3	$1.5/[(1-\alpha)^{-1/3}-1]$	$(1-2\alpha/3)-(1-\alpha)^{2/3}$
9	Diffusion, three-dimensional	D_4	$[1.5(1-\alpha)^{2/3}][1-(1-\alpha)^{1/3}]^{-1}$	$[1-(1-\alpha)^{1/3}]^2$
10	Diffusion, three-dimensional	D_5	$(3/2)(1+\alpha)^{2/3}[(1+\alpha)^{1/3}-1]^{-1}$	$[(1+\alpha)^{1/3}-1]^2$
11	Diffusion, three-dimensional	D_6	$(3/2)(1-\alpha)^{4/3}\{[1/(1-\alpha)^{1/3}]-1\}^{-1}$	$[1/(1-\alpha)^{1/3}-1]^2$
12	Contracted geometry shape (cylindrical symmetry)	R_2	$(1-\alpha)^{1/2}$	$2[1-(1-\alpha)^{1/2}]$
13	Contracted geometry shape (sphere symmetry)	R_3	$(1-\alpha)^{1/3}$	$3[1-(1-\alpha)^{1/3}]$
Acceleration curves				
14		P_1	1	α
15		P_2	$2\alpha^{1/2}$	$\alpha^{1/2}$
16		P_3	$(1.5)\alpha^{2/3}$	$\alpha^{1/3}$
17		P_4	$4\alpha^{3/4}$	$\alpha^{1/4}$
18		$P_{3/2}$	$2/3(\alpha)^{-1/2}$	$\alpha^{3/2}$
19		$P_{2/3}$	$3/2(\alpha)^{1/3}$	$\alpha^{2/3}$
29		$P_{3/4}$	$4/3(\alpha)^{-1/3}$	$\alpha^{3/4}$

N, nucleation; G growth.

Then, the master curves of the different models listed in Table I could be obtained with this function. Comparing the plots of $z(\alpha)$ calculated by eq. (7) using the experimental data with the master curves, we determined the mechanism of a solid-state process.

$\Delta S^{\#}$, $\Delta H^{\#}$, and $\Delta G^{\#}$ were calculated with the following equations:[20]

$$\Delta S^{\#} = 2.303\left(\log\frac{Ah}{kT_m}\right)R \tag{9}$$

$$\Delta H^{\#} = E - RT_m \tag{10}$$

$$\Delta G^{\#} = \Delta H^{\#} - T_m\Delta S^{\#} \tag{11}$$

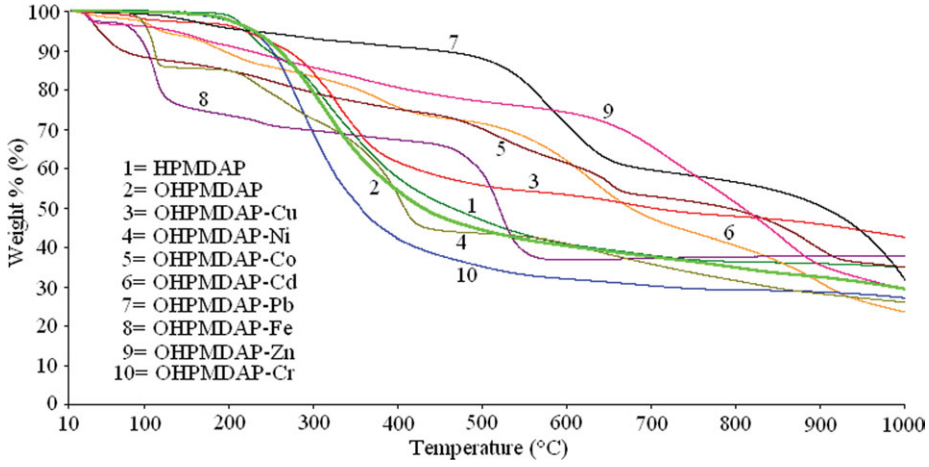

Figure 1. TGA curves of the monomer, oligomer, and oligomer–metal complex compounds. [Color figure can be viewed in the online issue, which is available at wileyonlinelibrary.com.]

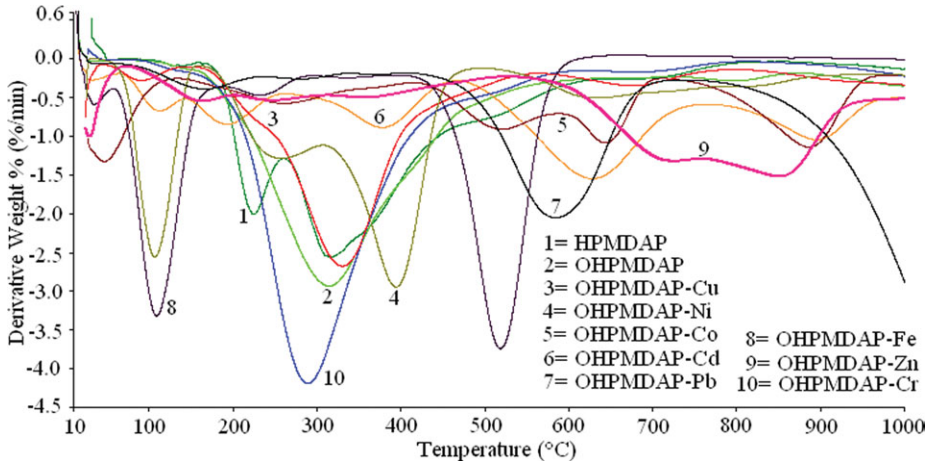

Figure 2. DTG curves of the monomer, oligomer, and oligomer–metal complex compounds. [Color figure can be viewed in the online issue, which is available at wileyonlinelibrary.com.]

In the previous equations, α, $g(\alpha)$, $f(\alpha)$, β, T_m, R, k, and h are the degree of reaction, integral function of conversion, a so-called kinetic function that depends on the reaction mechanism, heating rate, derivative thermogravimetric analysis (DTG) peak temperature, gas constant (8.314 J mol^{-1} K^{-1}), and the Boltzmann and Planck constants, respectively.

In this study, several methods based on a single heating rate were used in the thermal analysis. The linearization curves of the each decomposition step of the complexes were obtained with the least-squares method. The kinetic and thermodynamic parameters related to the HPMDAP, OHPMDAP, and OHPMDAP–metal complexes were calculated by software developed in our laboratory with the PHP Web programming language.[21]

RESULTS AND DISCUSSION

Thermal Stability

The thermodynamic and thermal properties of the HPMDAP, OHPMDAP, and OHPMDAP–metal complexes [where the metals were Ni(II), Cd(II), Cu(II), Fe(II), Zn(II), Co(II), Cr(III), and Pb(II)] were studied by thermogravimetric analysis (TGA) from ambient temperature to 1000°C in a nitrogen atmosphere. The TG/DTG curves and differential thermal analysis (DTA) profiles of the HPMDAP, OHPMDAP, and OHPMDAP–metal complexes are given in Figures 1–3, respectively. The thermal decomposition values, such as the initial and final temperatures, total mass losses, and temperatures corresponding to the maximum decomposition rate (DTG_{max}) for each step of the HPMDAP, OHPMDAP, and OHPMDAP–metal complex compounds, are given Table II. The curves obtained for most of the compounds examined were similar in character.

HPMDAP shows two decomposition stages in the temperature ranges 113–225 and 225–680°C and HPMDAP with 13.2 and 48.9% weight loss, respectively. The DTA profile exhibited two thermal effects at 150 and 226°C. The first peaks corresponded to the melting point of HPMDAP, whereas the last, at 226°C, corresponded to the decomposition of HPMDAP. From the TG

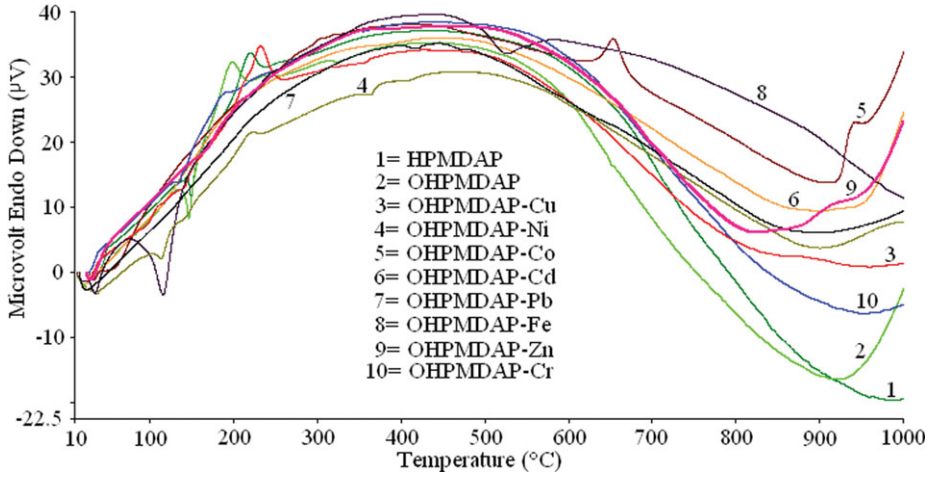

Figure 3. DTA curves of the monomer, oligomer, and oligomer–metal complex compounds. [Color figure can be viewed in the online issue, which is available at wileyonlinelibrary.com.]

Table II. Thermal Decomposition Values of the HPMDAP, OHPMDAP, and OHPMDAP–Metal Complex Compounds

Compound	Step	DTA peak (°C)	DTG_{max} (°C)	Temperature range (°C)	DTA	Mass loss (%)
HPMDAP	I	150, 226	231	113-225	Endo, exo	13.2
	II		323	225-680		48.9
	Residue			>680		35.7
OHPMDAP	I	147, 203	310	118-792	Endo, exo	70.7
	Residue			>792		29.3
OHPMDAP-Cd	I		116	78-148		5.09
	II		191	148-269		8.80
	III		377	269-485		13.3
	IV		630	485-765		29.4
	V		895	765-894		20.6
	Residue			>894		22.8
OHPMDAP-Zn	I	170	169	85-207	Endo	9.39
	II		257	207-324		7.31
	III		371	324-526		9.82
	IV		723	526-760		19.4
	V		855	760-955		25.3
	Residue			>955		28.8
OHPMDAP-Pb	I	419	176	81-240	Endo	6.21
	II		598	433-738		64.5
	Residue			>738		29.2
OHPMDAP-Ni	I	115, 143	109	88-137	Endo, endo	14.5
	II	237	261	137-315	Exo	17.2
	III	367	399	315-530	Endo	44.2
	Residue			>530		24.1
OHPMDAP-Fe	I	117	115	83-203	Endo	18.8
	II	533	524	422-629	Endo	44.9
	Residue			>629		37.8
OHPMDAP-Cu	I		102	456-150		3.30
	II		337	147-564		43.1
	III		683	564-840		10.9
	Residue			>840		42.7
OHPMDAP-Cr	I	138	296	103-617	Endo	73.5
	Residue			>617		26.5
OHPMDAP-Co	I		271	141-435		26.3
	II		526	432-601		13.7
	III	656	645	601-722	Exo	9.07
	IV		893	722-976		16.1
	Residue			>976		34.8

curve for OHPMDAP, it appeared that the sample decomposed in one stage over the temperature range 118–792°C. From the corresponding DTA profile, the endothermic and exothermic peaks for the polymer were noted. These peaks were found to be 147 and 203°C. Although the first peak at 147°C corresponded to the melting of OHPMDAP, the other peak at 203°C corresponded to the decomposition of OHPMDAP. The examination of the TG curve of OHPMDAP–Cd showed that the sample decomposed in five stages. Each decomposition stage for OHPMDAP–Cd occurred between 78 and 148 and at 148–269, 269–485, 485–765, and 765–894°C with mass losses 5.09, 8.8, 13.3, 29.4, 20.6 and 22.8%, respectively. The mass loss at the first stage with a mass loss of 5.09% was due to the dehydration of crystallization water from complex. On the other hand, OHPMDAP–Zn exhibited five decomposition stages, too. The DTA profile of OHPMDAP–Zn also showed one endothermic effect at 170°C. This endothermic peak corresponded to the melting of the OHPMDAP–Zn complex. The TG/DTG curves of

Table III. Kinetic Parameters of Thermal Degradation of All Compounds

Material	Stage	Method	$d\alpha/dt$ (1/s)	n	E (kJ/mol)	ln A (1/s)	$\Delta S^{\#}$ (kJ/mol K)	$\Delta H^{\#}$ (kJ/mol)	$\Delta G^{\#}$ (kJ/mol)	r
HPMDAP	I	MT	7.2712	0.2	31.6 ± 0.2	11.82	−150.9	27.46	103.3	0.99778
		vK	0.6661	0.3	31.0 ± 0.2	6.992	−191.1	26.83	122.9	0.99760
		MKN	0.0963	0.7	30.8 ± 0.7	5.007	−207.6	26.68	131.1	0.97379
		WHYC	0.0894	0.7	30.8 ± 0.2	4.932	−208.2	26.65	131.4	0.97373
		CR	0.0910	0.7	30.7 ± 0.1	4.934	−208.2	26.56	131.3	0.97359
		HM	3.4102	0.3	37.6 ± 0.2	10.20	−164.4	33.42	116.1	0.99629
	II	MT	15.648	2.7	70.2 ± 0.5	19.22	−90.88	65.33	119.5	0.98857
		vK	1.1252	3.1	69.1 ± 0.6	14.06	−133.7	64.16	143.8	0.98667
		HM	0.0469	3.4	64.5 ± 0.8	9.958	−167.9	59.57	159.6	0.98272
		MKN	0.0406	3.0	74.2 ± 0.1	11.77	−152.8	69.32	160.4	0.98463
		WYHC	0.0375	3.0	74.2 ± 0.1	11.69	−153.4	69.29	160.7	0.98460
		CR	0.0361	3.0	73.7 ± 0.1	11.55	−154.6	68.78	160.9	0.98435
OHPMDAP	I	vK	7.5606	1.1	21.3 ± 0.8	3.947	−217.8	16.45	145.1	0.98435
		MT	0.5537	0.8	22.3 ± 0.8	8.660	−178.6	17.43	123.0	0.97670
		HM	13.868	1.1	22.4 ± 0.3	9.491	−171.7	17.50	118.9	0.97061
		WHYC	0.0055	1.0	25.2 ± 0.5	−0.052	−251.1	20.33	168.7	0.97282
		MKN	0.0055	1.0	25.2 ± 0.5	−0.061	−251.2	20.34	168.8	0.97282
		CR	0.0268	1.2	19.0 ± 0.9	0.251	−248.5	14.12	161.0	0.92931
OHPMDAP-Cd	I	MT	10.347	2.0	110.0 ± 0.9	38.50	73.04	106.3	77.88	0.98283
		HM	2.4 10−7	2.0	110.0 ± 0.1	11.99	−147.4	107.0	164.4	0.98248
		vK	189.36	2.0	111.0 ± 0.4	41.73	99.84	107.3	68.48	0.98409
		MKN	3.7303	2.0	107.0 ± 0.2	34.25	37.67	103.2	88.63	0.98153
		WHYC	3.4537	2.0	107.0 ± 0.2	34.18	37.08	103.3	88.88	0.98152
		CR	3.5512	2.0	106.0 ± 0.2	34.15	36.84	103.1	88.79	0.98141
	II	HM	10.305	2.0	72.0 ± 0.1	11.40	−152.0	68.53	128.2	0.99070
		vK	0.0009	2.1	72.0 ± 0.8	22.54	−59.73	68.91	92.32	0.99020
		MT	56.777	1.9	71.0 ± 0.4	22.92	−56.58	68.07	90.24	0.98983
		MKN	0.2342	2.1	69.0 ± 1.0	16.32	−111.4	66.05	109.7	0.98728
		WHYC	0.2179	2.1	69.0 ± 1.0	16.24	−112.1	66.04	109.9	0.98726
		CR	0.2134	2.0	69.0 ± 1.0	16.14	−112.9	65.72	110.0	0.98712
	III	vK	82.075	1.1	89.0 ± 0.7	19.94	−85.66	83.22	139.3	0.98831
		CR	0.0132	1.2	86.0 ± 1.2	13.32	−140.7	80.75	172.9	0.98813
		MT	0.0136	1.1	93.0 ± 0.4	21.43	−73.23	87.29	135.2	0.97645
		WYHC	38.846	1.1	88.0 ± 1.0	11.80	−153.3	82.36	182.8	0.97577
		MKN	0.0816	1.1	88.0 ± 1.0	11.83	−153.0	82.40	182.6	0.97180
		HM	0.0167	1.2	88.0 ± 1.2	12.03	−151.4	82.35	181.5	0.97832
	IV	MT	152.32	1.3	114.0 ± 0.1	20.12	−86.87	106.5	185.5	0.99642
		vK	6.3075	1.4	113.0 ± 0.2	16.84	−114.1	105.8	209.5	0.99602
		HM	1393.8	1.2	115.0 ± 0.1	11.49	−158.6	107.1	151.4	0.99587
		MKN	0.1044	1.5	112.0 ± 0.5	12.51	−150.1	104.0	240.5	0.99387
		WHYC	0.0967	1.5	112.0 ± 0.5	12.43	−150.8	104.0	241.1	0.99386
		CR	0.0935	1.5	111.0 ± 0.5	12.31	−151.7	103.4	241.4	0.99380
	V	MT	236.16	1.1	313.5 ± 1.1	37.45	55.03	303.7	238.8	0.98156
		WYHC	0.0432	1.2	312.7 ± 1.9	28.76	−17.18	302.9	323.2	0.97649
		MKN	0.0467	1.2	312.6 ± 1.9	28.82	−16.66	302.8	322.4	0.97645
		vK	1.7 105	1.1	310.6 ± 1.4	43.76	107.5	300.8	174.0	0.97642
		CR	0,0449	1.2	312.1 ± 1.9	28.74	−17.35	302.3	322.8	0.97634

TABLE III. *Continued*

Material	Stage	Method	$d\alpha/dt$ (1/s)	n	E (kJ/mol)	ln A (1/s)	$\Delta S^{\#}$ (kJ/mol K)	$\Delta H^{\#}$ (kJ/mol)	$\Delta G^{\#}$ (kJ/mol)	r
		HM	6.8 10−4	0.8	308.6 ± 0.1	12.68	−150,8	298.8	476.7	0.97304
OHPMDAP-Co	I	MT	6.5400	1.1	43.1 ± 0.3	13.71	−135.8	38.57	112.4	0.96277
		WYHC	0.0108	1.0	40.8 ± 0.7	4.496	−212.5	36.36	152.0	0.96191
		MKN	0.0107	1.0	40.9 ± 0.7	4.508	−212.4	36.38	151.9	0.96191
		HM	2.8849	1.0	40.4 ± 0.1	9.992	−166.8	35.88	126.6	0.94158
		CR	0.0762	1.3	40.4 ± 0.9	6.359	−197.0	35.95	143.1	0.93651
		vK	2.2321	1.0	40.9 ± 0.6	9.846	−168.0	36.39	127.8	0.91976
	II	MT	9.5325	1.0	154.0 ± 0.8	27.74	−22.40	147.3	165.2	0.98580
		HM	0.0001	1.0	150.4 ± 0.1	11.46	−157.7	143.7	269.9	0.98488
		vK	146.20	1.0	148.9 ± 0.4	27.40	−25.25	142.2	162.5	0.97456
		WYHC	0.0104	1.0	152.8 ± 0.2	18.44	−99.78	146.2	226.0	0.97444
		MKN	0.0113	1.0	152.8 ± 0.2	18.52	−99.12	146.1	225.4	0.97580
		CR	0.0630	0.9	147.1 ± 0.2	19.38	−91.93	140.5	214.0	0.96496
	III	MT	70.420	3.0	433.0 ± 0.4	63.29	272.0	425.4	175.6	0.99833
		WYHC	0.1719	3.1	429.7 ± 1.1	54.54	199.3	422.1	239.1	0.99819
		MKN	0.1906	3.1	429.6 ± 1.1	54.63	199.9	421.9	238.4	0.99819
		CR	0.1855	3.1	429.5 ± 1.1	54.59	199.6	421.9	238.6	0.99818
		vK	5108.9	3.1	430.2 ± 1.3	69.51	323.7	422.6	125.4	0.99662
		HM	3,2 10−5	3.1	430.0 ± 0.1	13.80	−139.4	422.4	550.4	0.99585
	IV	MT	106.67	0.7	129.9 ± 0.2	18.67	−100.6	120.6	233.9	0.99566
		HM	0,0585	0.6	136.1 ± 0.1	11.83	−157.6	126.8	304.2	0.99542
		vK	3.6259	0.8	131.4 ± 0.2	15.45	−127.5	122.1	265.7	0.99500
		WYHC	0.0388	0.9	122.0 ± 0.5	9.901	−173.6	112.7	308.2	0.99296
		MKN	0.0418	0.9	122.1 ± 0.5	9.985	−172.9	112.7	307.5	0.99293
		CR	0.0368	0.9	121.3 ± 0.5	9.772	−174.7	111.9	308.6	0.99281
OHPMDAP-Ni	I	MT	7.4 10−9	2.3	272.4 ± 0.6	13.15	−137.6	269.30	322.0	0.99725
		HM	4.2 10−9	2.7	274.6 ± 0.1	13.15	−137.6	271.46	324.1	0.99725
		vK	4.8 10−7	2.4	270.4 ± 2.5	11.30	693.2	267.22	171.7	0.99713
		WYHC	0.0328	2.7	278.8 ± 1.6	84.37	454.6	275.69	101.5	0.99646
		MKN	0.0367	2.7	278.7 ± 1.6	84.45	455.2	275.59	101.2	0.99646
		CR	0.0345	2.7	278.9 ± 1.6	84.45	455.2	275.74	101.3	0.99646
	II	vK	0.6222	0.6	36.7 ± 0.1	7.792	−185.0	32.210	132.1	0.99555
		MT	4.2669	0.5	37.3 ± 0.1	12.57	−145.3	32.820	111.3	0.99418
		HM	2.9459	0.5	39.6 ± 0.1	10.07	−166.1	35.110	124.8	0.99195
		WYHC	0.0732	0.9	34.0 ± 0.4	5.045	−207.9	29.510	141.7	0.98984
		MKN	0.0751	0.9	33.9 ± 0.4	5.048	−207.9	29.420	141.6	0.98980
		CR	0.0655	0,8	33.6 ± 0.4	4.843	−209.6	29.110	142.3	0.98964
	III	MT	56.637	3.6	192.7 ± 0.1	40.83	87.84	187.21	128.3	0.99937
		HM	1.3 10−5	3.8	189.1 ± 0.1	13.24	−141.5	183.54	278.3	0.99946
		vK	60.749	3.8	190.8 ± 0.2	40.56	85.60	185.22	127.8	0.99925
		WYHC	0.5906	3.8	191.0 ± 0.4	33.66	28.22	185.42	166.5	0.99921
		MKN	0.6449	3.8	190.9 ± 0.4	33.73	28.87	185.39	166.0	0.99843
		CR	0.6157	3.8	190.6 ± 0.4	33.63	28.03	185.09	166.3	0.99821
OHPMDAP-Zn	I	MKN	0.0866	0.9	51.0 ± 1.3	12.09	−147.8	46.60	126.4	0.98766
		WYHC	0.0807	0.9	51.0 ± 1.3	12.02	−148.4	46.58	126.7	0.98765
		vK	1.0649	0.5	51.6 ± 1.8	14.77	−125.5	47.19	114.9	0.98751
		CR	0.0772	0.9	50.7 ± 1.3	11.89	−149.4	46.30	126.9	0.97624

TABLE III. *Continued*

Material	Stage	Method	$d\alpha/dt$ (1/s)	n	E (kJ/mol)	ln A (1/s)	$\Delta S^{\#}$ (kJ/mol K)	$\Delta H^{\#}$ (kJ/mol)	$\Delta G^{\#}$ (kJ/mol)	r
		HM	0.0042	0.5	56.6 ± 0.1	10.67	−159.6	52.19	138.3	0.95691
		MT	3.8774	0.7	54.1 ± 0.4	19.08	−89.64	49.64	98.04	0.93124
	II	MT	2.8249	1.0	107.6 ± 1.4	27.76	−17.46	103.8	111.7	0.98468
		WHYC	0.0069	1.0	106.8 ± 14	19.27	−88.08	103.0	142.7	0.98468
		MKN	0.0077	1.0	106.7 ± 1.1	19.35	−87.46	103.0	142.3	0.97468
		vK	30.082	1.1	104.8 ± 1.0	29.49	−3.071	101.0	102.4	0.97427
		HM	0.0001	1.0	105.6 ± 0.3	10.26	−162.9	101.8	175.2	0.96381
		CR	0.0440	1.1	103.3 ± 1.4	20.32	−79.36	99.64	135.3	0.95378
	III	MT	19.607	2.0	99.6 ± 0.2	22.81	−60.67	94.83	129.6	0.99408
		vK	6.8666	2.3	100.5 ± 0.5	21.94	−67.91	95.75	134.7	0.99397
		HM	0.0001	2.3	99.6 ± 0.1	11.27	−156.6	94.91	184.8	0.99264
		WHYC	0.0234	2.3	100.5 ± 0.8	16.26	−115.1	95.79	161.8	0.99188
		MKN	0.0253	2.3	100.5 ± 0.8	16.34	−114.4	95.80	161.5	0.99181
		CR	0.0231	2.3	100.1 ± 0.8	16.17	−115.9	95.33	161.8	0.99172
	IV	MT	26.112	0.7	140.4 ± 0.2	22.52	−67.74	132.0	200.2	0.98884
		WHYC	0.0261	1.0	151.4 ± 0.7	14.64	−133.2	143.0	277.1	0.98686
		MKN	0.0269	1.0	151.5 ± 0.7	14.68	−132.9	143.1	276.8	0.98686
		vK	4.4132	0.6	140.9 ± 0.4	18.50	−101.2	132.5	234.4	0.98598
		HM	0.0090	0.5	140.0 ± 0.1	12.20	−153.5	132.0	286.5	0.97716
		CR	0.0865	0.7	140.0 ± 0.7	14.46	−134.8	131.4	267.0	0.97404
	V	MT	192.75	1.3	333.1 ± 1.3	40.78	83.09	323.7	229.9	0.98575
		WHYC	0.0379	1.4	332.2 ± 0.3	32.15	11.38	322.8	310.0	0.98520
		MKN	0.0414	1.4	332.2 ± 0.3	32.24	12.07	322.8	309.1	0.98520
		vK	8678.6	1.3	343.3 ± 0.1	50.28	162.1	333.9	150.8	0.98510
		HM	1,2 10−6	1.3	333.7 ± 0.1	12.74	−150.4	324.3	493.7	0.97541
		CR	0.0395	1.4	331.7 ± 0.3	32.14	11.31	322.3	309.6	0.97517
OHPMDAP-Pb	I	MT	8.5717	0.8	29.3 ± 0.1	12.30	− 146.9	25.14	98.62	0.99835
		HM	5.8624	0.8	31.4 ± 0.1	10.18	−164.5	27.28	109.5	0.99175
		vK	2.1902	1.2	32.2 ± 0.1	9.414	−170.9	28.08	113.5	0.98849
		WYHC	0.0206	1.0	31.5 ± 0.2	4.568	−211.2	27.35	132.9	0.98770
		MKN	0.0208	1.0	31.5 ± 0.2	4.576	−211.1	27.36	132.9	0.98770
		CR	0.1206	1.2	28.5 ± 0.3	5.527	−203.2	24.34	125.9	0.98254
	II	HM	42.942	0.7	31.7 ± 0.1	10.44	−167.0	24.49	169.8	0.98720
		vK	0.5612	1.0	27.5 ± 0.3	3.228	−227.0	20.31	217.8	0.98569
		MT	17.710	1.0	28.7 ± 0.2	9.149	−177.7	21.50	176.1	0.98441
		WYHC	0.0126	1.0	28.5 ± 0.6	−0.431	−257.5	21.30	245.3	0.97441
		MKN	0.0125	1.0	28.5 ± 0.6	−0.442	−257.5	21.31	245.4	0.97441
		CR	0.0687	1.3	24.7 ± 1.1	0.733	−247.7	17.53	233.0	0.97954
OHPMDAP-Cr	I	HM	1.6935	1.4	40.5 ± 0.1	9.088	−174.7	35.76	135.3	0.98808
		MT	5.1357	1.2	41.1 ± 0.1	12.71	−144.6	36.36	118.8	0.98508
		vK	3.2988	1.4	41.4 ± 0.1	9.945	−167.6	36.66	132.2	0.96950
		MKN	0.0747	1.6	42.2 ± 0.7	6.327	−197.7	37.55	150.2	0.95600
		CR	0.0656	1.6	41.9 ± 0.7	6.133	−199.3	37.23	150.8	0.95559
		WYHC	0.0645	1.5	40.1 ± 0.6	5.736	−202.6	35.39	150.8	0.92933
OHPMDAP-Cu	I	MT	110.59	2.1	75.4 ± 0.3	28.89	−6.59	72.28	74.78	0.99722
		MKN	0.3885	2.2	71.6 ± 0.9	22.02	−63.75	68.49	92.39	0.99671
		WYHC	0.3586	2.2	71.6 ± 0.9	21.94	−64.38	68.50	92.63	0.99670
		CR	0.3682	2.2	71.3 ± 0.9	21.87	−64.95	68.27	92.62	0.99667

TABLE III. *Continued*

Material	Stage	Method	$d\alpha/dt$ (1/s)	n	E (kJ/mol)	ln A (1/s)	$\Delta S^{\#}$ (kJ/mol K)	$\Delta H^{\#}$ (kJ/mol)	$\Delta G^{\#}$ (kJ/mol)	r
		HM	0.0001	2.1	74.8 ± 0.1	11.51	−151.1	71.72	128.3	0.99394
		vK	1207.6	2.1	72.0 ± 1.0	30.19	4.222	68.94	67.35	0.99278
	II	MT	92.291	1.3	37.2 ± 0.2	11.86	−152.1	32.26	123.5	0.98678
		HM	15.900	1.3	37.7 ± 0.1	10.20	−165.8	32.74	132.2	0.98507
		vK	0.6548	1.5	36.4 ± 0.4	6.754	−194.5	31.48	148.2	0.97185
		WYHC	0.0843	1.7	33.2 ± 0.7	4.074	−216.8	28.26	158.3	0.95011
		MKN	0.1037	1.7	36.1 ± 0.8	4.852	−210.4	31.12	157.3	0.94844
		CR	0.0820	1.7	34.2 ± 0.7	4.243	−215.4	29.27	158.5	0.94842
	III	MT	127.25	1.5	146.6 ± 0.3	23.31	−60.28	139.1	193.3	0.99438
		HM	0.0761	1.6	144.7 ± 0.8	15.65	−123.9	137.2	248.8	0.99281
		vK	13.320	1.7	140.7 ± 0.9	20.31	−85.23	133.2	209.9	0.99281
		WYHC	0.0650	1.7	140.8 ± 0.9	15.00	−129.3	133.3	249.8	0.99203
		MKN	0.0704	1.7	140.8 ± 0.9	15.08	−128.7	133.4	249.2	0.99202
		CR	0.0634	1.7	140.2 ± 0.9	14.90	−130.1	132.7	249.9	0.99193
OHPMDAP–Fe	I	MT	35.700	1.6	73.5 ± 1.0	26.36	−28.12	70.23	81.48	0.98566
		HM	0.0001	1.8	73.3 ± 0.3	10.90	−156.6	70.05	132.7	0.98427
		vK	841.49	1.8	74.5 ± 0.9	29.83	0.701	71.25	70.97	0.97496
		WYHC	0.1131	1.8	74.9 ± 2.7	21.04	−72.36	71.58	100.5	0.97465
		MKN	0.1226	1.8	74.9 ± 2.7	21.12	−71.76	71.58	100.2	0.97465
		CR	0.1215	1.8	74.8 ± 2.7	21.08	−72.03	71.52	100.3	0.97464
	II	MT	235.53	1.5	27.5 ± 0.1	9.612	−173.2	20.92	159.4	0.99317
		HM	380.62	1.3	30.8 ± 0.1	10.59	−164.9	24.20	156.2	0.95975
		WYHC	0.0115	1.3	23.0 ± 0.2	−0.991	−261.3	16.40	225.4	0.99077
		MKN	0.0113	1.3	23.0 ± 0.2	−1.004	−261.4	16.41	225.6	0.99070
		CR	0.0778	1.8	20.3 ± 0.2	0.510	−248.8	13.66	212.7	0.98252
		vK	0.5005	1.8	29.6 ± 0.07	3.775	−221.7	22.96	200.3	0.98212

r, correlation coefficient; $d\alpha/dt$, reation rate.

OHPMDAP–Pb and OHPMDAP–Fe exhibited two decomposition stages. The first decomposition stage for OHPMDAP–Pb occurred between 81 and 240°C with a mass loss of 6.21%. The last decomposition step occurred in the temperature range 433–738°C. Each decomposition stage for OHPMDAP–Fe occurred between 83 and 203°C and at 422–629°C with mass losses of 18.8 and 44.9%. The DTA profiles of this complexes showed three endothermic peaks at 117, 419, and 533°C. The peaks at 117 and 533°C corresponded to the decomposition of OHPMDAP–Fe. The peak at 419°C was due to the melting of OHPMDAP–Pb. OHPMDAP–Ni decomposed at 88°C. The mass loss at the first stage in the temperature range 88–137°C with a mass loss 14.5%, corresponding to the elimination of H_2O from the complex. It was shown that this complex is also melting at 143°C in the DTA curve. OHPMDAP-Cu shows three decomposition stages in the temperature ranges 456–150°C, 147–564°C and 564–840°C with 3.30%, 43.1%, and 10.9% weight losses, respectively. The carbon residue at 1000°C was found to be 42.7%. According to The TG/DTG curves of OHPMDAP–Co exhibited four decomposition stages. Also, the OHPMDAP–Cr complex decomposed in one stage and melted at 138°C. According to TGA, although the initial decomposition temperature of HPMDAP was lower than OHPMDAP, it was more stable than HPMPDA because of the long conjugated band systems. OHPMDAP–Cu demonstrated a higher thermal stability than HPMDAP, OHPMDAP, and the other OHPMDAP–metal complex compounds. Also, to check the thermal stability of the complexes in the solid state, the initial temperatures of the decomposition of all of the compounds were compared. We found that the thermal stabilities of HPMDAP, OHPMDAP, and

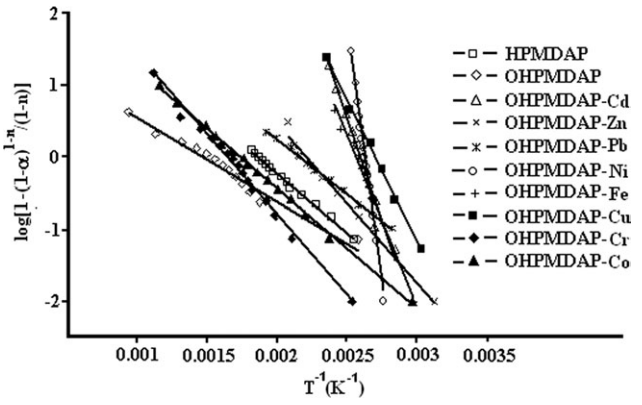

Figure 4. MT plots of the first decomposition stage of HPMDAP, OHPMDAP, and all of the OHPMDAP–metal complexes.

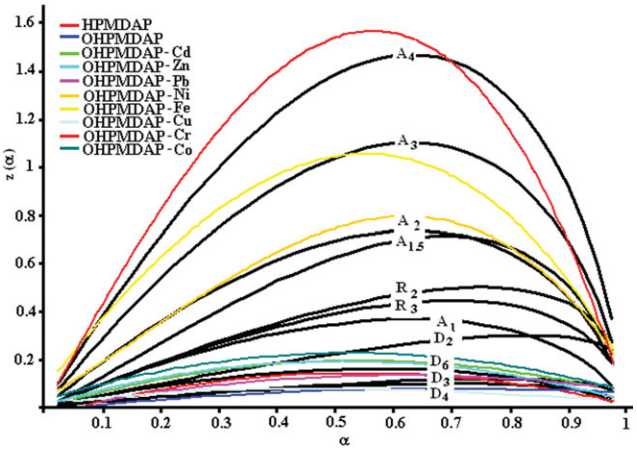

Figure 5. Master curves of $z(\alpha)$ and the experimental data. [Color figure can be viewed in the online issue, which is available at wileyonlinelibrary.com.]

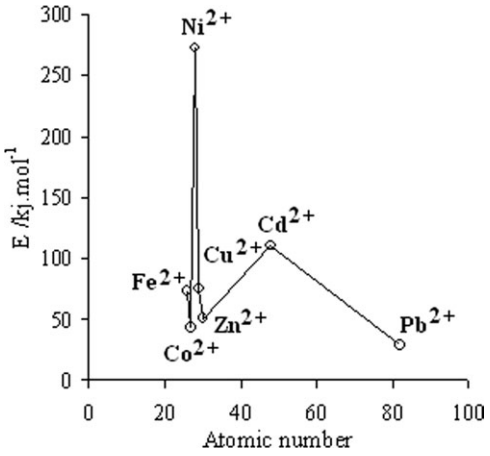

Figure 6. E values of the divalent metal ions of the complexes versus the atomic number: the first decomposition stage.

the other OHPMDAP–metal complex compounds followed the order OHPMDAP–Cu > OHPMDAP–Co > OHPMDAP > HPMDAP > OHPMDAP–Cr > OHPMDAP–Ni > OHPMDAP–Zn > OHPMDAP–Fe > OHPMDAP–Pb > OHPMDAP–Cd. In our previous study, we reported that the thermal stabilities of *N*, *N*′-bis(3,5-di-*t*-butylsalicylideneimine)-1,3-propanediamine complexes of cobalt, nickel, iron, and copper increased in the following sequence: Ni(II) > Cu(II) > Co(II) > Fe(II).[22] Then, in another study, we determined that the thermal stabilities of the metal complexes of the oligo-2-[(4-morpholin-4-ylphenyl)imino]methylphenol were in the following sequence: Cu(II) > Co(II) > Zn(II) > Zr(II) > Pb(II) > Cd(II).[10] As expected, these results clearly show that the thermal stabilities of the complexes increased as the ionic radii decreased.

Kinetic and Thermodynamic Study

The TGA experiments were performed to determine the thermal behavior of the HPMDAP, OHPMDAP, and OHPMDAP–metal complexes and to suggest decomposition processes and kinetic parameters. The CR, HM, vK, MKN, MT, and WHYC methods were used for the kinetic analysis. These methods were based on a single heating rate. From the TG curves, n, E, $\Delta S^{\#}$, $\Delta H^{\#}$, $\Delta G^{\#}$, and A and the linearization curves of the thermal degradation of all of the materials were elucidated by the methods mentioned previously. The results obtained are given in Table III. The E values of the first decomposition stage obtained from Arrhenius plots by the best methods for the HPMDAP, OHPMDAP, and OHPMDAP–metal complexes (see the MT plots given in Figure 4 for the first decomposition step of all of the compounds). The E values of the first decomposition stage of OHPMDAP complexes of Cd(II), Co(II), Ni(II), Zn(II), Pb(II), Cr(III), Cu(II), and Fe(II) were 110.0 ± 0.9 kJ/mol according to the MT method, 43.1 ± 0.3 kJ/mol according to the MT method, 272.4 ± 0.6 kJ/mol according to the MT method, 51.0 ± 1.3 kJ/mol according to the MKN method, 29.3 ± 0.1 kJ/mol according to the MT method, 40.5 ± 0.1 kJ/mol according to the HM method, 75.4 ± 0.3 kJ/mol according to the MT method, and 73.5 ± 1.0 kJ/mol according to the MT method, respectively. According to these results, we found that the E values of the complexes for the first decomposition stage followed the order $E_{\text{OHPMDAP–Ni}} > E_{\text{OHPMDAP–Cd}} > E_{\text{OHPMDAP–Cu}} >$

Table IV. Kinetic Function Relations to the HPMPDAP, OHPMPDAP, and OHPMPDAP–Metal Complexes

	Step				
Compound	I	II	III	IV	V
HPMDAP	D_4	D_4			
OHPMDAP	D_6				
OHPMDAP-Cd	D_6	D_4	D_4	D_3	D_3
OHPMDAP-Zn	D_6	D_4	D_4	D_3	D_6
OHPMDAP-Pb	D_6	D_4			
OHPMDAP-Ni	A_2	D_4	D_6		
OHPMDAP-Fe	A_3	D_4			
OHPMDAP-Cu	D_4	D_6	D_4		
OHPMDAP-Cr	A_4				
OHPMDAP-Co	D_6	D_4	D_4	D_4	

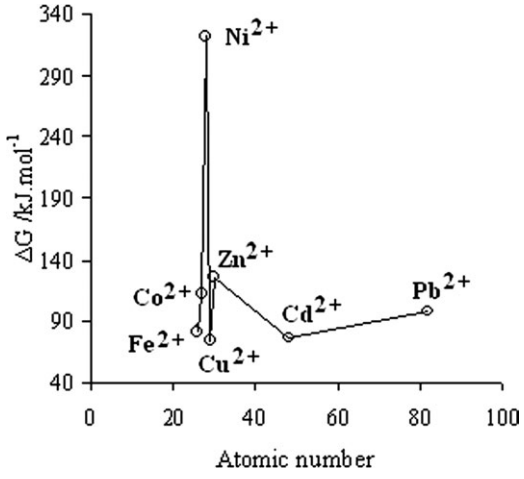

Figure 7. $\Delta G^{\#}$ values of the divalent metal ions of the complexes versus the atomic number: the first decomposition stage.

Applied Polymer SCIENCE

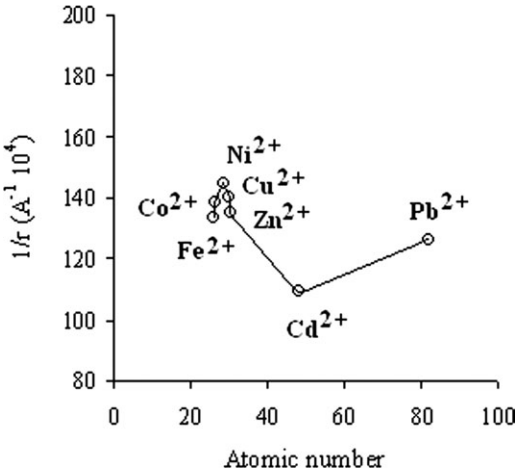

Figure 8. Reciprocals of the ionic radii of the divalent metal ions versus the atomic number.

$E_{OHPMDAP–Fe} > E_{OHPMDAP–Zn} > E_{OHPMDAP–Co} > E_{OHPMDAP–Cr} > E_{OHPMDAP–Pb} > E_{HPMDAP} > E_{OHPMDAP}$, respectively.

According to the kinetic data obtained from the DTG curves, several complexes had negative entropies of activation, which indicated that the studied complexes had more ordered systems than the reactants. For all of methods, the determination of A and n was possible from the expression of $g(\alpha)$ in eq. (3) and $n \neq 1$:

$$g(\alpha) = \frac{1-(1-\alpha)^{1-n}}{1-n}$$

The results were in good agreement with the values obtained from all of them. The results indicate that the values from all of the methods were comparable. As shown in Table III, the value of correlation coefficients of linearization curves of HPMDAP, OHPMDAP and OHPMDAP–metal complexes are approximately 1.00 and values of ns are around 1.00 for OHPMDAP, OHPMDAP–Zn, OHPMDAP–Pb complexes. The kinetic data obtained by different methods agree with each other. The $\Delta H^{\#}$, $\Delta S^{\#}$, and $\Delta G^{\#}$ values of all the complexes material were calculated with eqs. (9), (10), and (11). The thermodynamic parameters calculated were reported in Table III. Also Table III represents maximum decomposition rate calculated by integral methods based on one heating rate, for each stage of solid state decomposition of all the material. According to this, the pre-exponential factor obtained by Arrhenius plot in the temperature range studied for each material significantly affects the maximum decomposition rate and $\Delta S^{\#}$ According to Table III the values of E and A calculated from CR, MKN and WHYC are very close to each other. As a result of this, the values of thermodynamic parameters are compatible with the other. Although the E values obtained by HM, VK and MT methods are almost same, corresponding values of A are different from each other and the result affects the other thermodynamic values, importantly. This issue is still very much discussed in the literature. In several articles, the existence of these different kinetic triplets [E, A, and $g(\alpha)$], especially the values of A, from various kinetic equations of the same class are explained by the different approximations used in the methods.[23–26]

On the other hand, we have employed reference theoretical master curves to find out the reaction mechanism for the studied systems. According to Criado et al.,[17] a master plot is a characteristic curve independent of the condition of the measurement. The master curve plots of $z(\alpha)$ versus α for different mechanisms have been illustrated in Figure 5. The mechanism functions related to the thermal decomposition processes are given in Table IV. The experimental data of $z(\alpha)$ for the OHPMDAP and OHPMDAP–metal complexes agreed very well with the D_n values, which corresponded to a deceleration mechanisms and the A_n master curve. The OHPMDAP and OHPMDAP–metal complexes are generally D_n mechanisms. The E and $\Delta G^{\#}$ (Figures 6 and 7) changed with increasing atomic number in the third series of d block elements for the OHPMDAP–metal complexes. The complexes of Cu(II), Ni(II), Fe(II), and Cd(II) with OHPMDAP were present in the peaks of the energy curve. This means that these complexes were more stable at the beginning of decomposition than those on the bottom of the curve, the Co(II), Cr(III), Zn(II), and Pb(II) complexes. To determine the thermal stability of the complexes in the solid state, the initial temperatures of the decomposition of the complexes were compared. A plot of the initial decomposition temperatures of the complexes and the corresponding reciprocal ionic radii of the divalent metal ions against the atomic number is shown in Figures 8 and 9. As shown in these figures, the thermal stabilities of the complexes increased in general as the ionic radii of the metal decreased. It was clear that the thermal stability of the OHPMDAP–Cu complex was greater than those of the others.

CONCLUSIONS

Several analysis methods based on one heating rate were used to analyze the single set of data for the thermal decomposition of the HPMDAP, OHPMDAP, and OHPMDAP–metal complexes. The thermal data obtained were evaluated with the CR, HM, vK, MKN, MT, and WHYC methods and with the Criado–Malek–Ortega method for kinetic analysis. The E values obtained with the CR, HM, vK, MKN, MT, and WHYC methods were in good

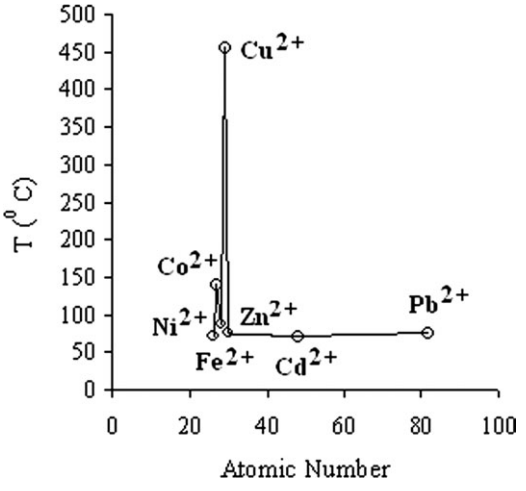

Figure 9. Values of the initial decomposition temperature versus the atomic number.

agreement with one another. An analysis of the experimental results suggested that the actual decomposition mechanisms of the HPMDAP, OHPMDAP, and OHPMDAP–metal complex compounds were generally a decelerated D_n and sigmoidal A_n type. We found that the thermal stabilities and E values of the HPMPDAP, OHPMPDAP, and OHPMPDAP–metal complex compounds for the first decomposition stage followed the following order, respectively: OHPMDAP–Cu > OHPMDAP–Co > OHPMDAP > HPMDAP > OHPMDAP–Cr > OHPMDAP–Ni > OHPMDAP–Zn > OHPMDAP–Fe > OHPMDAP–Pb > OHPMDAP–Cd and $E_{OHPMDAP–Ni} > E_{OHPMDAP–Cd} > E_{OHPMDAP–Cu} > E_{OHPMDAP–Fe} > E_{OHPMDAP–Zn} > E_{OHPMDAP–Co} > E_{OHPMDAP–Cr} > E_{OHPMDAP–Pb} > E_{HPMDAP} > E_{OHPMDAP}$.

REFERENCES

1. Chan, W. *Coord. Chem. Rev.* **2007**, *251*, 2104.
2. Kaya, I.; Dogan, F.; Bilici, A. *Polym. Int.* **2009**, *58*, 570.
3. Antony, R.; Tembe, G. L.; Ravindranathan, M.; Ram, R. N. *Polymer* **1998**, *18*, 4327.
4. Chantarassiri, N.; Tuntulani, T.; Tongroung, P.; Seangprasertkit, R.; Wannarong, W. *Eur. Polym. J.* **2000**, *36*, 695.
5. Cazacu, M.; Marcu, M.; Vlad, A.; Rusu, G. I.; Avadane, M. *J. Organomet. Chem.* **2004**, *689*, 3005.
6. Oriol, L.; Alonso, P. J.; Martinez, J. I.; Pidol, M.; Serrano, J. L. *Macromolecules* **1994**, 27, 1869.
7. Mart, H. *Des. Monomers Polym.* **2006**, *9*, 551.
8. Doğan, F.; Kaya, İ.; Bilici, A.; Sacak, M. *J. Appl. Polym. Sci.* **2010**, *118*, 547.
9. Kaya, İ.; Bilici, A. *J. Appl. Polym. Sci.* **2007**, *105*, 1356.
10. Doğan, F.; Kaya, İ. *Des. Monomers Polym.* **2007**, *10*, 527.
11. Coats, A. W.; Redfern, J. P. *Nature* **1964**, *201*, 68.
12. Horowitz, H. H.; Metzger, G. *Anal. Chem.* **1963**, *35*, 1464.
13. Madhusudanan, P. M.; Krishnan, K.; Ninan, K. N. *Thermochim. Acta* **1993**, *221*, 13.
14. Van Krevelen, D. W.; Herden, C.; Huntjons, F. *J. Fuel* **1951**, *30*, 253.
15. Wanjun, T.; Yuwen, L.; Hen, Z.; Cunxin, W. *Thermochim. Acta* **1993**, *408*, 39.
16. MacCallum, J. R.; Tanner, J. *Eur. Polym. J.* **1970**, *6*, 1033.
17. Criado, J.; Malek, J.; Ortega, A. *Thermochim. Acta* **1989**, *147*, 377.
18. Kaya, İ.; Bilici, A.; Saçak, M. *Polimery* **2009**, *54*, 106.
19. Senum, G. I.; Yang, K. T. *J. Therm. Anal.* **1977**, *11*, 445.
20. Al-Wallan, A. A. *Synth. React. Inorg. Met.-Org. Chem.* **2002**, *32*, 489.
21. Doğan, F. Ph.D. Thesis, Ege University, **2006**.
22. Doğan, F.; Ulusoy, M.; Öztürk, Ö.; Kaya, İ.; Salih, B. *J. Therm. Anal. Calorim.* **2009**, *96*, 267.
23. Orfao, J. J. M. *AlChE J.* **2007**, *53*, 2905.
24. Pérez-Maqueda, L. A.; Criado, J. M. *J. Therm. Anal. Calorim.* **2000**, *60*, 909.
25. Flynn, J. H., *Thermochim. Acta* **1997,** *300*, 83.
26. Deng, C.; Cai, J.; Liu, R. *Solid State Sci.* **2009**, *11*, 1375.